Title

Novel Nitro-PAH Formation from Heterogeneous Reactions of PAHs with NO2, NO3/N2O5, and OH Radicals: Prediction, Laboratory Studies, and Mutagenicity

Journal

Environmental Science and Technology, 48(1)

ISSN

0013-936X

Authors

Jariyasopit, Narumol
McIntosh, Melissa
Zimmermann, Kathryn
et al.

Publication Date

2014-01-07

DOI

10.1021/es4043808

Peer reviewed

Published in final edited form as:
Environ Sci Technol. 2014 January 7; 48(1): 412–419. doi:10.1021/es4043808.

Novel Nitro-PAH Formation from Heterogeneous Reactions of PAHs with NO_2, NO_3/N_2O_5, and OH Radicals: Prediction, Laboratory Studies and Mutagenicity

NARUMOL JARIYASOPIT[1], **MELISSA MC INTOSH**[1], **KATHRYN ZIMMERMANN**[2], **JANET AREY**[2], **ROGER ATKINSON**[2], **PAUL HA-YEON CHEONG**[1], **RICH G. CARTER**[1], **TIAN-WEI YU**[3], **RODERICK H. DASHWOOD**[3], and **STACI L. MASSEY SIMONICH**[1,4]

[1]Department of Chemistry, Oregon State University, Corvallis, Oregon USA 97331

[2]Air Pollution Research Center, University of California, Riverside

[3]Institute of Biosciences & Technology, Texas A&M Health Science Center, Houston, Texas, USA, 77030

[4]Environmental and Molecular Toxicology, Oregon State University, Corvallis, Oregon, USA, 97331

Abstract

The heterogeneous reactions of benzo[a]pyrene-d_{12} (BaP-d_{12}), benzo[k]fluoranthene-d_{12} (BkF-d_{12}), benzo[ghi]perylene-d_{12} (BghiP-d_{12}), dibenzo[a,i]pyrene-d_{14} (DaiP-d_{14}), and dibenzo[a,l]pyrene (DalP) with NO_2, NO_3/N_2O_5, and OH radicals were investigated at room temperature and atmospheric pressure in an indoor Teflon chamber and novel mono NO_2-DaiP, and mono NO_2-DalP products were identified. Quartz fiber filters (QFF) were used as a reaction surface and the filter extracts were analyzed by GC/MS for nitrated-PAHs (NPAHs) and tested in the Salmonella mutagenicity assay, using *Salmonella typhimurium* strain TA98 (with and without metabolic activation). In parallel to the laboratory experiments, a theoretical study was conducted to rationalize the formation of NPAH isomers based on the thermodynamic stability of OH-PAH intermediates, formed from OH-radical-initiated reactions. NO_2 and NO_3/N_2O_5 were effective oxidizing agents in transforming PAHs to NPAHs, with BaP-d_{12} being the most readily nitrated. Reaction of BaP-d_{12}, BkF-d_{12} and BghiP-d_{12} with NO_2 and NO_3/N_2O_5 resulted in the formation of more than one mono-nitro isomer product, while the reaction of DaiP-d_{14} and DalP resulted in the formation of only one mono-nitro isomer product. The direct-acting mutagenicity increased the most after NO_3/N_2O_5 exposure, particularly for BkF-d_{12} in which di-NO_2-BkF-d_{10} isomers were measured. The deuterium isotope effect study suggested that substitution of deuterium for hydrogen lowered both the direct and indirect acting mutagenicity of NPAHs and may result in an underestimation of the mutagencity of the novel NPAHs identified in this study.

*Corresponding author staci.simonich@orst.edu; phone: (541) 737-9194; fax: (541) 737-0497 .

Supporting Information Available This material is available free of charge via the Internet at http://pubs.acs.org.

Introduction

Nitrated polycyclic aromatic hydrocarbons (NPAHs) are PAH derivatives emitted directly to the atmosphere from combustion sources and/or formed from atmospheric transformation via homogeneous gas-phase OH- and NO_3-radical initiated reactions of PAHs,[1] and some NPAHs are more mutagenic than the parent PAHs.[2, 3] Gas-phase reactions of PAHs to form NPAHs are initiated by either OH or NO_3 radical attack at the position of highest electron density on the aromatic ring, followed by NO_2 addition with subsequent loss of H_2O or HNO_3, respectively. In contrast, heterogeneous nitration may follow a different mechanism and previous studies have shown that heterogeneous reactions of pyrene and fluoranthene with NO_3/N_2O_5 yield different nitropyrene and nitrofluoranthene isomers than do the corresponding gas-phase reactions.[4-7] The kinetics of heterogeneous reactions vary significantly due to the inherent complexity of heterogeneous reactions caused by the characteristics of the substrates, surface chemistry and the substrate-specific kinetics of heterogeneous reactions.[8-11] The formation of NPAHs from the heterogeneous reactions of PAHs containing two to five rings has been studied with NO_2, N_2O_5,[5-7, 10, 12-15] whereas a limited number of studies have investigated the formation of NPAHs from the heterogeneous reaction of PAHs with more than five aromatic rings.[16] In field studies, nitrobenzopyrenes and nitroperylene (MW297) were the highest molecular weight NPAHs detected in the atmosphere.[17, 19-20]

The objectives of this study were to 1) identify NPAHs, including novel NPAHs, formed from the heterogeneous reaction of filter-sorbed, low volatility perdeuterated PAHs with NO_2, NO_3/N_2O_5, and OH radicals using laboratory experiments and theoretical calculations and 2) associate NPAH formation in the laboratory experiments with the mutagenicity of the extracts. Five higher molecular weight PAHs, including benzo[a]pyrene-d_{12} (BaP-d_{12}), benzo[k]fluoranthene-d_{12} (BkF-d_{12}), benzo[ghi]perylene-d_{12} (BghiP-d_{12}), dibenzo[a,i]pyrene-d_{14} (DaiP-d_{14}), and dibenzo[a,l]pyrene (DalP) were selected for this research because of their mutagenicity[21, 22] and the lack of data on their formation of NPAH products during heterogeneous reactions. Deuterated PAHs were used for the experiments, except for DalP for which the deuterated analog was not commercially available, because they are not present in the environment and allowed us to attribute the formation of deuterated nitro PAH products solely to the reactions in the chamber. Because the mutagenicity of deuterated nitro PAH products may differ from non-deuterated analogs, a deuterium isotope effect study was carried out to investigate the effect of perdeuteration on mutagenicity. To our knowledge, NPAH products of DalP and DaiP have not been previously identified.

Experimental

Chemicals and Materials

Perdeuterated BaP-d_{12}, BkF-d_{12}, BghiP-d_{12}, and DaiP-d_{14} were purchased from CDN Isotopes (Point-Claire, Quebec, Canada) and Cambridge Isotope Laboratories (Andover, MA). Because perdeuterated DalP was not commercially available we purchased the non-deuterated DalP from Cambridge Isotope Laboratories (Andover, MA). Dichloromethane, ethyl acetate and dimethyl sulfoxide were purchased from Fisher Scientific (Santa Clara,

CA) and EMD Chemicals (Gibbstown, NJ). Salmonella tester strain TA98 was originally purchased from Xenometrix, Inc. Of the mono-NO_2-PAH and di-NO_2-PAH products identified in this study, only 6-NO_2-BaP-d_{11} was commercially available and was purchased from Chiron AS (Trondheim, Norway). Details of the synthesis of 7-nitrobenzo[k]fluoranthene, 3,7-dinitrobenzo[k]fluoranthene, 7-nitrobenzo[ghi]perylene and 5-nitrobenzo[ghi]perylene are given in Supporting Information (SI).

Spiked Filter Preparation and Exposures

Heterogeneous reactions of particulate-bound PAHs have been observed in chamber studies and in the ambient atmosphere[5-7, 23]. In this study, the quartz fiber filters (QFFs) (8 in x 10 in, No.1851-865, Tisch Environmental, Cleves, OH) were pre-baked (350°C) before use. Each clean QFF was cut into 4 quarters. Ten μg of the individual PAHs in ethyl acetate were deposited separately onto each quarter of the QFFs with a pipette and placed in the laboratory fume hood, allowing ethyl acetate to evaporate at room temperature for approximately 30 minutes. A quarter of clean, unspiked QFF was also placed in the chamber during each experiment as a negative control for toxicological and chemical studies.

Laboratory experiments were carried out in ~7000 L indoor collapsible Teflon chamber equipped with two parallel banks of black lamps and a Teflon-coated fan at room temperature (~297 K) and ~740 Torr.[7] All the filters were placed on a standing, rotating apparatus inside the Teflon chamber.[5] Details of how NO_2, NO_3/N_2O_5, and OH radicals were generated are given in SI.

Sample extraction and Analysis

The QFFs were extracted twice with pressurized liquid extraction and dichloromethane using an extraction method previously described in detail[18] and both extracts were combined. The extracts that were subjected to chemical analysis were evaporated and solvent-exchanged to ethyl acetate under a purified N_2 stream with a Turbovap II (Caliper Life Sciences, MA). The extracts subjected to the Salmonella assay were evaporated to dryness under a stream of N_2 and the residue was dissolved in 500 μl of dimethylsulfoxide (DMSO). The extracts from the unexposed filters, that had been spiked with individual PAH, were split in half based on solvent weight. One half of the extract was prepared for mutagenicity testing and the other half was prepared for chemical analysis.

The analyses of parent PAHs and NPAHs in the analytical extracts were conducted using gas chromatographic mass spectrometry (GCMS, Agilent 6890 GC coupled with an Agilent 5973N MSD) in selected ion monitoring (SIM) and scan modes using both electron impact (EI) and negative chemical ionization (NCI) (using CH_4 as the reagent gas), with a programmed temperature vaporization (PTV) inlet (Gerstel, Germany). A 5% phenyl substituted methylpolysiloxane GC column (DB-5MS, 30m×0.25mm I.D., 0.25 μm film thickness, J&W Scientific, USA) was used to separate the parent PAHs and NPAHs.

Theoretical Study

In parallel to the laboratory experiments, a theoretical study was conducted using Density Functional Theory (DFT), with the B3LYP functional and the 6-31G(d) basis set, as

implemented in Gaussian03. The thermodynamic stability of the OH-PAH intermediates was used to rationalize the formation of NPAH isomers. From our computations, we used the thermodynamic stability of various isomeric OH-PAH intermediates to predict the regioselectivity of heterogeneous nitration (see discussion below).

Salmonella Mutagenicity Assay

The basic method followed that reported by Maron and Ames[24] and *Salmonella typhimurium* strain TA98 was used in the study. The experimental details have been described elsewhere.[18] The positive control doses were 2 μg of 2-aminoanthracene (2-AA) and 20 μg of 4-nitro-1,2-phenylenediamine (NPD) for assays with and without metabolic activation (rat S9 mix), respectively. The negative control (DMSO) dose was 30 μl. All filter extracts were tested in triplicate.

Results and Discussion

Theoretical Studies

The mechanism of gas-phase OH radical-initiated reaction with PAHs to give NPAH has been previously described.[1, 4, 7, 25, 26] Scheme 1 shows that, in the gas-phase, the initial addition of OH radical to an aromatic ring leads to an OH-PAH adduct. This radical may react with NO_2 to yield a nitrocyclohexadienyl radical intermediate, followed by water elimination to form the NPAH. Alternatively, in ambient atmospheres, the OH-PAH adduct can also react with O_2 to give other products.[26]

To verify our computation strategy, computations for pyrene and fluoranthene were carried out and compared with nitro products identified in a previous gas-phase OH-radical chamber study[4] (Table SI.1). Positions 1 and 3 on pyrene and fluoranthene, respectively, were found to yield the most thermodynamically stable OH-PAH adduct intermediates (pyrene:ΔG_{rxn} = −18.4 kcal/mol and fluoranthene: ΔG_{rxn} = −16.7 kcal/mol) (Table SI.1). Followed by NO_2 addition to the *ortho* position, the reactions were predicted to yield 2-nitropyrene and 2-nitrofluoranthene as major NPAH products from the OH radical-initiated gas-phase reaction of pyrene and fluoranthene, respectively. The good agreement between the computed and experimental results[4] for pyrene and fluoranthene suggested that the thermodynamic stability of the OH-PAH adducts in the first step of the gas-phase OH radical-initiated reaction could be used to predict the formation of NPAHs in the gas-phase.

The strong thermodynamic stability of intermediates formed from addition to 1 and 3 positions on pyrene and fluoranthene, respectively, dictates all reactions. Therefore, addition of NO_2 by direct nitration reactions should also occur at the same positions. Unlike the gas-phase radical-initiated reactions, the heterogeneous nitration of pyrene and fluoranthene with N_2O_5[6] and NO_2[12, 27] formed 1-nitropyrene and 3-nitrofluoranthene as dominant isomers. Although the isomer distributions of nitropyrenes and nitrofluoranthenes can be used to distinguish between the radical-initiated and heterogeneous reactions and possible reaction mechanisms have been previously discussed [5-6, 13, 28], the reaction mechanism of heterogeneous nitration has not been unequivocally identified. Table 1 shows the calculated free energies of the OH-PAH adducts for all possible OH radical attack positions at

peripheral aromatic carbons and predicts the NPAHs formed from heterogeneous reaction of BaP, BkF, BghiP, DaiP, and DalP. The optimized geometries and energies of the studied PAHs and intermediates are given in the SI.

NPAH Product Identification

All major NPAH product isomers, with peak height in the GC chromatograms greater than three times the noise peak height, were identified based on the GC retention time and full scan EI and/or NCI mass spectra of the standards when they were commercially available. In addition, we synthesized 7-nitrobenzo[k]fluoranthene, 3,7-dinitrobenzo[k]fluoranthene, 7-nitrobenzo[ghi]perylene and 5-nitrobenzo[ghi]perylene because they were not commercially available (see the SI). Table 1 lists the NPAHs identified in the laboratory exposure experiments and whether or not they had been previously detected in the environment.

For NPAH isomers without available standards, a previously published method was used to predict their GC retention time orders.[29] White et al. found that the dipole moment of mononitro PAH isomers predicted their GC retention time order on a non-polar SE-52 GC column, a 5% phenyl substituted methylpolysiloxane stationary phase, with the NPAH isomers eluting in order of increasing dipole moment.[29] In this study, we predicted the GC retention time orders of the most stable mono-nitro PAH isomers products listed in Table 1 by calculating their dipole moments using Gaussian with B3LYP/6-31G(d) (Table SI.2) and predicted the molecular ion of the NCI mass spectra based on their molecular weight.

Benzo[a]pyrene—Figures SI.1A-C show the NCI full scan chromatograms of BaP-d_{12}exposed to NO_2, NO_3/N_2O_5, and OH radical overlaid with the chromatogram of the unexposed BaP-d_{12}. The m/z 264 peak is the molecular ion of BaP-d_{12}. Because the extracts from the unexposed filters were split, in some cases, the parent PAH peaks in the unexposed extracts had lower abundances than those in the exposed extracts. BaP-d_{12} reacted with NO_2 and NO_3/N_2O_5 (Figures SI.1A and SI.1B) and yielded significant amounts of mono NO_2-BaP-d_{11} isomers. In contrast, after the OH radical exposures, noticeably lower amounts of mono NO_2-BaP-d_{11} products were formed (Figures SI.1C). Three mono NO_2-BaP-d_{11} isomers (Figures SI.1A-C, peaks 1-3) were identified from the reaction of BaP-d_{12} with NO_2, NO_3/N_2O_5, and OH radicals (Table 1). No dinitro PAH isomers were identified in the BaP-d_{12} exposures. Based on the ΔG values shown in Table 1, we predicted that the most reactive position for OH attack of BaP was 6, followed by 1 and 3, respectively. This prediction was consistent with a previous study which determined the distribution of NO_2-BaP isomers based on the calculated reactivity numbers.[30] The calculated dipole moments of these isomers suggested a GC retention time order of 6-, 1- and 3-NO_2-BaP-d_{11} (Table SI.2) and this same retention time order was previously observed for these isomers using the same type of nonpolar GC column.[31] Therefore, the earliest eluting peak with m/z 308 (Figures SI.1A and SI.1B, peak 1) was identified as 6-NO_2-BaP-d_{11} and its retention time was confirmed with a standard of 6-NO_2-BaP-d_{11}. This peak had the highest peak height (~20-490 times higher than 1- and 3-NO_2-BaP-d_{11}), in both EI and NCI, and corresponded to the highest stability of the calculated 6-OH-BaP adduct (Table 1). In addition, 6-NO_2-BaP was recently identified as a major product from the heterogeneous reaction of BaP coated soot particles with NO_2.[14] A slight difference in dipole moments of 1- and 3-NO_2-BaP-d_{11}

(6.06 and 6.16 Debye, respectively) predicted close GC retention times for these two isomers and peaks 2 and 3 (both with m/z 308) were tentatively assigned to 1- and 3-NO_2-BaP-d_{11}, respectively. 1- and 3-NO_2-BaP were previously found to be minor products from a study of heterogeneous reaction of BaP with NO_2 and N_2O_5.[8, 12] However, to date, 1- and 3-NO_2-BaP have not been measured in the environment (Table 1).

Benzo[k]fluoranthene—Figures SI.2A-C show the NCI full scan chromatograms of BkF-d_{12} exposed to NO_2, NO_3/N_2O_5, and OH radical overlaid with the chromatogram of the unexposed BkF-d_{12}. The m/z 264 peak is the molecular ion of BkF-d_{12}. Two mono NO_2-BkF-d_{11} peaks (m/z 308), 3- and 7-NO_2-BkF-d_{11}, were identified from the reaction of BkF-d_{12} with NO_2 (Figure SI.2A) based on the ΔG values shown in Table 1. The weaker calculated dipole moment of 7-NO_2-BkF-d_{11}, relative to 3-NO_2-BkF-d_{11}, suggested it would elute first. The retention time of 7-NO_2-BkF-d_{11} was confirmed with the non-deuterated 7-NO_2-BkF standard, noting a slight difference in retention times due to the deuterium isotope effect. Therefore, peaks 1 and 2 were identified as 7-NO_2-BkF-d_{11} and 3-NO_2-BkF-d_{11}, respectively. The formation of 3-NO_2-BkF-d_{11} was expected to be more favorable than 7-NO_2-BkF-d_{11} based on the stability of the various OHBkF adducts (Table 1). However, the intensity of the 3-NO_2-BkF-d_{11} peak was significantly lower than that of 7-NO_2-BkF-d_{11}. The same observation was made in the EI full scan chromatogram and may suggest that 3-NO_2-BkF-d_{11} was more prone to further nitration, yielding di-NO_2-BkF-$d_{10,}$ compared to 7-NO_2-BkF-d_{11}. BkF-d_{12} was nitrated during the NO_3/N_2O_5 exposure and five mono-NO_2-BkF-d_{11} products (m/z 308) were tentatively identified in the NCI full scan chromatogram (Figure SI.2B). As shown in Table 1, the predicted order of product formation, based on the thermodynamic stability of the OH-BkF adducts, was: 3, 7, 8, 1 and 9 positions of mono-NO_2-BkF-d_{11}. Based on the calculated dipole moments of these compounds, the predicted GC retention time elution order was: 7-, 1-, 8-, 3- and 9-NO_2-BkF-d_{11} (Table SI.2). It should be noted that all of the extracts were also run in SIM mode and the mono-NO_2-BaP-d_{11} peaks were baseline resolved in the selected ion chromatograms (data not shown).

In addition to the mono-NO_2-BkF-d_{11} products, di-NO_2-BkF-d_{10} products (m/z 352) were also identified after the NO_3/N_2O_5 exposure (Figure SI.2B). Dinitro-PAHs are believed to form from reaction of mono-nitro PAHs with the oxidizing agent[5, 13] and, therefore, the predicted most abundant mono-NO_2-BkF-d_{11} product (3-NO_2-BkF-d_{11}), with the most stable OH-BkF-d_{11} intermediate, was most likely to further react with an oxidizing agent. To predict the most likely di-NO_2-BkF-d_{10} products, we calculated the thermodynamic stability of the OH-3-NO_2-BkF-d_{10} adducts. If 3-NO_2-BkF-d_{11} were the only mono-NO_2-BkF-d_{11} isomer that underwent further nitration, the five dominant di-NO_2-BkF-d_{10} products were predicted to be: 3,12-, 3,7-, 3,4-, 3,6- and 3,8-NO_2-BkF-d_{10} (Figure SI.3). Because 3-NO_2-BkF-d_{11} was not the only mono-NO_2-BkF-d_{11} product formed, other di-nitro-BkF-d_{10} isomers may also have been formed. The positive identification of these di-NO_2-BkF-d_{10} products required authentic standards which were not commercially available. Only the identity of 3,7-NO_2-BkF-d_{10} (peak 11) was confirmed with the non-deuterated 3,7-NO_2-BkF standard.

The OH radical exposure chromatograms indicated the presence of 7, 3, 8, and 1-NO_2-BkF-d_{11}, but not 9-NO_2-BkF-d_{11} (Figure SI.2C). The NCI full scan chromatograms for OH

radical exposures showed traces of other degradation products, possibly oxygenated PAHs, mostly eluting before the mono-NO_2-BkF-d_{11} and di-NO_2-BkF-d_{10} isomers (Figures SI.2C). To date, the mono-NO_2-BkF and di-NO_2-BkF isomers identified in this study have not been measured in the environment (Table 1).

Benzo[ghi]perylene—Unlike the other PAHs, BghiP-d_{12} was not effectively nitrated by NO_2 and only one small unidentified peak (m/z 483) was observed in the NCI full scan chromatogram (Figure SI.4A). In contrast, after NO_3/N_2O_5 exposure, three apparent mono-NO_2-BghiP-d_{11} isomers (m/z 332) were identified (Figure SI.4B). Based on the ΔG values shown in Table 1, we predicted that 5-, 7-, and 4-NO_2-BghiP-d_{11} would be the most abundant mono-NO_2-BghiP-d_{11} products. A previous study also identified 5-NO_2-BghiP as a dominant nitro product formed from the reaction of BghiP adsorbed on silica gel particles with NO_2.[16] The calculated dipole moments suggested a retention time elution order of 7-, 4-, and 5-NO_2-BghiP-d_{11} (Table SI.2). After OH radical exposure, only 5-NO_2-BghiP-d_{11}, the predicted most abundant NO_2-BghiP-d_{11}isomer, was identified in the NCI full scan chromatogram (Figure SI.4C). To date, the mono-NO_2-BghiP isomers identified in this study have not been measured in the environment (Table 1).

Dibenzo[a,i]pyrene—As shown in Figures SI.5A and SI.5B, the NO_2 and NO_3/N_2O_5 exposures resulted in only one mono-NO_2-DaiP-d_{13} product (m/z 360). Based on the ΔG values shown in Table 1, we predicted that 5-NO_2-DaiP-d_{13} would be the most abundant mono-NO_2-DaiP-d_{13} product. To date, 5-NO_2-DaiP has not been measured in the environment (Table 1). The exposure of DaiP-d_{14} to OH radicals did not result in any mono-NO_2-DaiP-d_{13} products (Figures SI.5C).

Dibenzo[a,l]pyrene—Because a perdeuterated DalP standard was not commercially available, we used a nondeuterated DalP standard for our experiments. The presence of DalP in a blank exposed filter was below the detection limit. A single mono-NO_2-DalP peak (m/z 347) was observed after the NO_2 and NO_3/N_2O_5 exposures (Figure SI.6A and SI.6B). Based on the ΔG values shown in Table 1, we predicted that 6-NO_2-DalP would be the most abundant mono-NO_2-DalP product and, to date, 6-NO_2-DalP has not been measured in the environment (Table 1). Similarly, OH radical exposure also resulted in the formation of a single mono-NO_2-DalP peak (m/z 347), likely 6-NO_2-DalP, but to a much lesser extent than the NO_2 and NO_3/N_2O_5 exposures (Figure SI.6C).

Estimated Effectiveness of Nitration—The percent of NPAH product formation relative to the amount of unexposed parent PAH was calculated and used to estimate the effectiveness of nitration for the different PAHs tested, under the various exposure conditions. We estimated the percent of nitro product formation from the sum of identified NPAH product peak areas (in exposed extracts) to its parent PAH peak area (in unexposed extracts) from the EI full scan chromatograms (Table SI.3). These values should be considered rough estimates because the objective of this research was to qualitatively identify nitro products and not quantitatively determine their concentrations (there was no surrogate addition for quantitation). BaP-d_{12} was the most readily nitrated, in comparison to the other PAHs tested, by the NO_2, NO_3/N_2O_5 and OH radical exposures (90%, 41%, and

20%, respectively), while BghiP-d_{12} was the least effectively nitrated (Table SI.3). Among the various exposures, the percent NPAH product formation was highest for the NO_2 exposures.

Salmonella Mutagenicity Assay

Spontaneous revertant counts of DMSO (30 μl) alone were ~25/plate for both assays. The mutagenicity of the chamber air system was tested by placing clean filters in all chamber experiments. In the assays without S9, the revertant counts for the blank filters were 27, 38, and 28 revertants/plate for the NO_2, NO_3/N_2O_5, and OH exposures, respectively. In the assays with S9, the revertant counts for the blank filters were 44, 42, and 35 revertants/plate for the NO_2, NO_3/N_2O_5, and OH exposures, respectively. Overall, they were comparable to the spontaneous revertant counts. This shows that the chamber environment and our sample preparation process had no substantial effect on the mutagenicity results. The split extracts of the unexposed filters, containing ~1 nmol of the individual PAHs tested, resulted in 43 to 65 revertants/plate and 24 to 49 revertants/plate for the assays with and without S9, respectively (Figure 1).

Direct-acting mutagenicity—Many NPAHs are direct-acting mutagens, independent of metabolic activation[32]. Figure 1A shows the means and standard errors of the direct-acting mutagenicity of the various exposure extracts. The direct-acting mutagenicity increased the most after NO_3/N_2O_5 exposure, particularly for BkF-d_{12}. For all of the PAHs tested, the NO_3/N_2O_5 exposure resulted in 6- to 432-fold increase in the direct-acting mutagenicity. The sharp increase in the direct-acting mutagenicity of the NO_3/N_2O_5 exposed BkF-d_{12} (432-fold) extract may correspond to the formation of the di-NO_2-BkF-d_{10} products. The dose-response profiles of two non-deuterated NO_2-BkF standards indicated that 3,7-NO_2-BkF is a strong direct-acting mutagen, whereas 7-NO_2-BkF is not (Figure SI.7A). Higher mutagenic activities of di-NO_2-PAH-d_{10} products, in comparison to mono-nitro isomers, were reported for dinitropyrenes in which their direct-acting mutagenicity, in TA98, was 272- to 467-fold higher than that of 1-nitropyrene.[33]

The increases in the direct-acting mutagenicity of BaP-d_{12} were less pronounced after exposure to NO_2 and OH radicals, compared to the NO_3/N_2O_5 exposure where the direct-acting mutagenicity increased by 43-fold (Figure 1A). This sharp increase was due to the formation of 1- and 3-NO_2-BaP-d_{11} products, rather than the formation of 6-NO_2-BaP-d_{11} because 6-NO_2-BaP-d_{11} contains a nitro group perpendicular to the aromatic moiety.[34] Previous studies suggested that NPAHs with a perpendicular orientation of the NO_2 group relative to the aromatic plane, have a high first half-wave reduction potential, which restricts the nitro-reduction process by bacteria.[33, 34] A mixture of 1-NO_2-BaP and 3-NO_2-BaP was previously found to be 2.5 fold more mutagenic with TA98, than 6-NO_2-BaP.[8] Some studies have reported that 1- and 3-NO_2-BaP were direct-acting mutagens in a Salmonella assay, but 6-NBaP was not.[35, 36] In a more recent study, 1- and 3-NO_2-BaP were found to induce 713 and 1,931 revertants/nmol, respectively, in TA98, while 6-NO_2-BaP induced less than 1 revertant/nmol.[33] However, the direct-acting mutagenicity of the NO_2 exposed BaP-d_{12} extract was surprisingly low given that the same mono-NO_2-BaP-d_{11} products were measured as in the NO_3/N_2O_5 exposure (Figures 1A and SI.1A) and the percent NPAH

formation was the highest (Table SI.3). We confirmed that this was not due to cytotoxicity. Therefore, the relatively high direct-acting mutagenicity of the NO_3/N_2O_5 exposed BaP-d_{12} extract may have been caused by the formation of other, yet unidentified, products.

For BghiP-d_{12}, the direct-acting mutagenicity of the NO_2 exposed extract was not significantly different from the unexposed extract. This finding was consistent with the chemical analysis which showed insignificant NPAH formation after the NO_2 exposure. However, there were 97 and 12-fold increases in the direct-acting mutagenicity after BghiP-d_{12} was exposed to NO_3/N_2O_5 and OH radicals, respectively (Figure 1A), corresponding to the formation of mono-NO_2-BghiP-d_{11} products. Of the three identified mono-NO_2-BghiP-d_{11} products, 7-NO_2-BghiP-d_{11} is expected to contribute the least to the direct-acting mutagenicity due to the NO_2 orientation (Table SI.4). Dose-response profiles of non-deuterated 5-NO_2-BghiP and 7-NO_2-BghiP standards showed that both were non-mutagenic (< 1 rev/nmol) (Figure SI.7).

Changes in direct-acting mutagenicity of DaiP-d_{14} and DalP with the different exposures were less pronounced than the other PAHs tested (Figure 1A), suggesting that the single nitro product formed did not exhibit strong direct-acting mutagenicity. The orientation of nitro groups in both 5-NO_2-DaiP-d_{14} and 6-NO_2-DalP, identified as the major products from all exposures, are nearly perpendicular to the aromatic plane (Table SI.4) and may cause these products to be less mutagenic.

Indirect-acting mutagenicity—Unsubstituted PAHs are known to be indirect-acting mutagens which require metabolic activation to express mutagenicity and unreacted parent PAHs may contribute to the indirect-acting mutagenicity of exposed extracts. In addition, not all NPAHs are direct-acting mutagens. For example, 6-NO_2-BaP was previously found to be an indirect-acting mutagen[36, 37] and some NPAHs, including 1-NO_2-BaP and 3-NO_2-BaP, exhibit both direct- and indirect-acting mutagenicity.[36] As shown in Figure 1B, the overall indirect-acting mutagenicity profile was similar to the directing-acting mutagenicity profile, with increased indirect-acting mutagenicity after the NO_3/N_2O_5 exposures. This shows that NO_3/N_2O_5 are not only strong oxidants in transforming PAHs to NPAHs, but also in forming potential direct and indirect-acting mutagens. In particular, BaP-d_{12}, BkF-d_{12}, and BghiP-d_{12} were degraded to both strong direct-acting and strong indirect-acting mutagenic products. BkF-d_{12} and BghiP-d_{12} were the only two compounds that induced indirect-acting mutagenic activities significantly higher than the background after OH radical exposure (Figure 1B and Figure SI.8B). Dose-response profiles of non-deuterated 7-NO_2-BkF and 3,7-NO_2-BkF standards showed that the 3,7-NO_2-BkF exhibited both direct- and indirect-acting mutagenicity (96 and 513 rev/nmol, respectively), while 7-NO_2-BkF was not mutagenic in either assay (Figure SI.7). This implies that the presence of the five di-NO_2-BkF-d_{11} products in the NO_3/N_2O_5 exposed extract contributed significantly to the direct-acting mutagenicity, as well as the indirect-acting mutagenicity. On the other hand, 5-NO_2-BghiP was mutagenic to TA98 with S9 (27 rev/nmol), while 7-NO_2-BghiP was not (Figure SI.7).

Deuterium Isotope Effect on Mutagenicity—The results from the deuterium isotope effect mutagenicity studies of BaP/BaP-d_{12}, 6-NO_2-BaP/6-NO_2-BaP-d_{11}, PYR/PYR-d_{10} and

1-NO_2-PYR/1-NO_2-PYR-d_9 are shown in Figures SI.9A-D and Figures SI.10A-D. ANOVA analysis was carried out to determine the statistical significance of differences between deuterated and nondeuterated pairs of PAHs. There was no statistically significant deuterium isotope effect (ANOVA, $P > 0.05$) for the parent BaP/BaP-d_{12} and PYR/PYR-d_{10} in the direct acting mutagenicity assay (Figures SI.9A and SI.10A). However, a statistically significant deuterium isotope effect (ANOVA, $P < 0.05$) was observed for 6-NO_2-BaP/6-NO_2-BaP-d_{11} and 1-NO_2-PYR/1-NO_2-PYR-d_9 (Figures SI.9C and SI.10C) in the direct acting mutagenicity assay. While 6-NO_2-BaP exhibited a weak direct-acting mutagenicity, the activity of 6-NO_2-BaP-d_{11} was comparable to the background response (Figure SI.9C). GC/MS analysis of the 6-NO_2-BaP standard, with both EI and NCI, showed no contamination of 3- and/or 1-NO_2-BaP. However, both 1-NO_2-PYR and 1-NO_2-PYR-d_9 were direct acting mutagens. The difference in the magnitudes of the deuterium isotope effect on the direct-acting mutagenicity of 1-NO_2-PYR/1-NO_2-PYR-d_9 and 6-NO_2-BaP/6-NO_2-BaP-d_{11} cannot be explained by this study alone. Additional studies on other NPAHs and/or the use of different bacterial strains may help to understand the difference in the metabolic pathways.

In the indirect acting mutagenicity assay, no statistically significant deuterium isotope effect was observed for the parent BaP/BaP-d_{12} and PYR/PYR-d_{10} (ANOVA, $P > 0.05$) (Figure SI.9B and SI.10B). However, a statistically significant deuterium isotope effect was observed for 6-NO_2-BaP/6-NO_2-BaP-d_{11} and 1-NO_2-PYR/1-NO_2-PYR-d_9 in the indirect acting mutagenicity assay (ANOVA, $P < 0.05$) and substitution of deuterium for hydrogen lowered the mutagenicity (Figures SI.9D and SI.10D). Overall, the deuterium isotope effect study suggested that substitution of deuterium for hydrogen lowered the direct and indirect acting mutagenicity of NPAHs and may result in an underestimation of the mutagencity of the novel NPAHs identified in this study. Further discussion is provided in the SI.

Supplementary Material

Refer to Web version on PubMed Central for supplementary material.

Acknowledgments

This publication was made possible in part by grant number P30ES00210 from the National Institute of Environmental Health Sciences (NIEHS), NIH and NIEHS Grant P42 ES016465, and the U.S. National Science Foundation (ATM-0841165). Its contents are solely the responsibility of the authors and do not necessarily represent the official view of the NIEHS, NIH. Salmonella assays were conducted in the Cancer Chemoprotection Program (CCP) Core Laboratory of the Linus Pauling Institute, Oregon State University.

References

1. Atkinson R, Arey J. Atmospheric Chemistry of Gas-Phase Polycyclic Aromatic Hydrocarbons: Formation of Atmospheric Mutagens. Environ. Health Perspect. 1994; 102:117–126. [PubMed: 7821285]
2. Durant JL, Lafleur AL, Plummer EF, Taghizadeh K, Busby WF, Thilly WG. Human Lymphoblast Mutagens in Urban Airborne Particles. Environ. Sci. Technol. 1998; 32:1894–1906.
3. Purohit V, Basu AK. Mutagenicity of Nitroaromatic Compounds. Chem. Res. Toxicol. 2000; 13:673–692. [PubMed: 10956054]

4. Atkinson R, Arey J, Zielinska B, Aschmann SM. Kinetics and Nitro-Products of the Gas-Phase OH and NO_3 Radical-Initiated Reactions of Naphthalene-d8, Fluoranthene-d10, and Pyrene. Int. J. Chem. Kinet. 1990; 22:999–1014.
5. Zimmermann K, Jariyasopit N, Massey Simonich SL, Tao S, Atkinson R, Arey J. Formation of Nitro-PAHs from the Heterogeneous Reaction of Ambient Particle-Bound PAHs with $N_2O_5/NO_3/NO_2$. Environ. Sci. Technol. 2013; 47:8434–8442. [PubMed: 23865889]
6. Zielinska B, Arey J, Atkinson R, Ramdahl T, Winer AM, Pitts JN. Reaction of dinitrogen pentoxide with fluoranthene. J. Am. Chem. Soc. 1986; 108:4126–4132.
7. Zimmermann K, Atkinson R, Arey J, Kojima Y, Inazu K. Isomer distributions of molecular weight 247 and 273 nitro-PAHs in ambient samples, NIST diesel SRM, and from radical-initiated chamber reactions. Atmos. Environ. 2012; 55:431–439.
8. Pitts JN Jr, Van Cauwenberghe KA, Grosjean D, Schmid JP, Fitz DR, Belser W, Knudson G, Hynds PM. Atmospheric reactions of polycyclic aromatic hydrocarbons: facile formation of mutagenic nitro derivatives. Science (New York, NY). 1978; 202:515–519.
9. Zelenyuk A, Imre D, Beránek J, Abramson E, Wilson J, Shrivastava M. Synergy between secondary organic aerosols and long-range transport of polycyclic aromatic hydrocarbons. Environ. Sci. Technol. 2012; 46:12459–12466. [PubMed: 23098132]
10. Kamens RM, Guo J, Guo Z, McDow SR. Polynuclear aromatic hydrocarbon degradation by heterogeneous reactions with N_2O_5 on atmospheric particles. Atmos. Environ. 1990; 24:1161–1173.
11. Esteve W, Budzinski H, Villenave E. Relative rate constants for the heterogeneous reactions of NO_2 and OH radicals with polycyclic aromatic hydrocarbons adsorbed on carbonaceous particles. Part 2: PAHs adsorbed on diesel particulate exhaust SRM 1650a. Atmos. Environ. 2006; 40:201–211.
12. Pitts JN, Sweetman JA, Zielinska B, Atkinson R, Winer AM, Harger WP. Formation of nitroarenes from the reaction of polycyclic aromatic hydrocarbons with dinitrogen pentoxide. Environ. Sci. Technol. 1985; 19:1115–1121. [PubMed: 22288761]
13. Miet K, Le Menach K, Flaud PM, Budzinski H, Villenave E. Heterogeneous reactivity of pyrene and 1-nitropyrene with NO_2: Kinetics, product yields and mechanism. Atmos. Environ. 2009; 43:837–843.
14. Carrara M, Wolf J-C, Niessner R. Nitro-PAH formation studied by interacting artificially PAH-coated soot aerosol with NO_2 in the temperature range of 295-523 K. Atmos. Environ. 2010; 44:3878–3885.
15. Pitts JN Jr, Zielinska B, Sweetman JA, Atkinson R, Winer AM. Reactions of adsorbed pyrene and perylene with gaseous N_2O_5 under simulated atmospheric conditions. Atmos. Environ. 1985; 19:911–915.
16. Delmas S, Muller JF. Use of FTMS laser microprobe for the in situ characterization of nitro-PAHs on particles. Analusis. 1992; 20:165–170.
17. Bamford HA, Baker JE. Nitro-polycyclic aromatic hydrocarbon concentrations and sources in urban and suburban atmospheres of the Mid-Atlantic region. Atmos. Environ. 2003; 37:2077–2091.
18. Wang W, Jariyasopit N, Schrlau J, Jia Y, Tao S, Yu T-W, Dashwood RH, Zhang W, Wang X, Simonich SLM. Concentration and Photochemistry of PAHs, NPAHs, and OPAHs and Toxicity of $PM_{2.5}$ during the Beijing Olympic Games. Environ. Sci. Technol. 2011; 45:6887–6895. [PubMed: 21766847]
19. Albinet A, Leoz-Garziandia E, Budzinski H, Villenave E. Polycyclic aromatic hydrocarbons (PAHs), nitrated PAHs and oxygenated PAHs in ambient air of the Marseilles area (South of France): Concentrations and sources. Sci. Total Environ. 2007; 384:280–292. [PubMed: 17590415]
20. Hattori T, Tang N, Tamura K, Hokoda A, Yang X, Igarashi K, Ohno M, Okada Y, Kameda T, Toriba A. Particulate polycyclic aromatic hydrocarbons and their nitrated derivatives in three cities in Liaoning Province, China. Environ. Forensics. 2007; 8:165–172.

21. USEPA. Development of a Relative Potency Factor (RPF) Approach for Polycyclic Aromatic Hydrocarbon (PAH) Mixtures, an external review draft. U.S. Environmental Protection Agency, Intergrated Risk Information System (IRIS); Washington, DC: 2010.
22. Devanesan PD, Cremonesi P, Nunnally JE, Rogan EG, Cavalieri EL. Metabolism and mutagenicity of dibenzo [a, e] pyrene and the very potent environmental carcinogen dibenzo [a, l] pyrene. Chem. Res. Toxicol. 1990; 3:580–586. [PubMed: 2103330]
23. Pitts JN Jr, Zielinska B, Sweetman JA, Atkinson R, Winer AM. Reactions of adsorbed pyrene and perylene with gaseous N_2O_5 under simulated atmospheric conditions. Atmos. Environ. 1967; 19:911–915.
24. Maron DM, Ames BN. Revised methods for the Salmonella mutagenicity test. Mutat. Res. 1983; 113:173–215. [PubMed: 6341825]
25. Pitts JN Jr, Sweetman JA, Zielinska B, Winer AM, Atkinson R. Determination of 2-nitrofluoranthene and 2-nitropyrene in ambient particulate organic matter: Evidence for atmospheric reactions. Atmos. Environ. 1985; 19:1601–1608.
26. Zimmermann K, Atkinson R, Arey J. Effect of NO_2 Concentration on Dimethylnitronaphthalene Yields and Isomer Distribution Patterns from the Gas-Phase OH Radical-Initiated Reactions of Selected Dimethylnaphthalenes. Environ. Sci. Technol. 2012; 46:7535–7542. [PubMed: 22757668]
27. Miet K, Le Menach K, Flaud PM, Budzinski H, Villenave E. Heterogeneous reactivity of pyrene and 1-nitropyrene with NO_2: Kinetics, product yields and mechanism. Atmos. Environ. 2009; 43:837–843.
28. Gross S, Bertram AK. Reactive uptake of NO_3, N_2O_5, NO_2, HNO_3, and O_3 on three types of polycyclic aromatic hydrocarbon surfaces. J. Phys. Chem. A. 2008; 112:3104–3113. [PubMed: 18311955]
29. White C, Robbat A, Hoes R. Gas chromatographic retention characteristics of nitrated polycyclic aromatic hydrocarbons on SE-52. Chromatographia. 1983; 17:605–612.
30. Dewar M, Mole T, Urch D, Warford E. 689. Electrophilic substitution. Part IV. The nitration of diphenyl, chrysene, benzo [a] pyrene, and anthanthrene. J. Chem. Soc. 1956:3572–3575.
31. Bamford HA, Bezabeh DZ, Schantz MM, Wise SA, Baker JE. Determination and comparison of nitrated-polycyclic aromatic hydrocarbons measured in air and diesel particulate reference materials. Chemosphere. 2003; 50:575–587. [PubMed: 12685733]
32. Fu PP. Metabolism of nitro-polycyclic aromatic hydrocarbons. Drug Metab. Rev. 1990; 22:209–268. [PubMed: 2272288]
33. Jung H, Heflich RH, Fu PP, Shaikh AU, Hartman P. Nitro group orientation, reduction potential, and direct-acting mutagenicity of nitro-polycyclic aromatic hydrocarbons. Environ. Mol. Mutagen. 1991; 17:169–180. [PubMed: 2022194]
34. Fu PP, Qui FY, Jung H, Von Tungeln LS, Zhan DJ, Lee MJ, Wu YS, Heflich RH. Metabolism of isomeric nitrobenzo[a]pyrenes leading to DNA adducts and mutagenesis. Mutat. Res. 1997; 376:43–51. [PubMed: 9202737]
35. Chou M, Heflich R, Casciano D, Miller D, Freeman J, Evans F, Fu P. Synthesis, spectral analysis, and mutagenicity of 1-, 3-, and 6-nitrobenzo [a] pyrene. J. Med. Chem. 1984; 27:1156–1161. [PubMed: 6381731]
36. Pitts JN Jr, Zielinska B, Harger WP. Isomeric mononitrobenzo [a] pyrenes: synthesis, identification and mutagenic activities. Mutat. Res. 1984; 140:81–85. [PubMed: 6540365]
37. Rosenkranz, HS.; Mermelstein, R. The mutagenic and carcinogenic properties of nitrated polyclic aromatic hydrocarbons. White, CM., editor. Huethig; Heidelberg: 1985. p. 267-297.
38. Schauer C, Niessner R, Pöschl U. Analysis of nitrated polycyclic aromatic hydrocarbons by liquid chromatography with fluorescence and mass spectrometry detection: air particulate matter, soot, and reaction product studies. Anal. Bioanal. Chem. 2004; 378:725–736. [PubMed: 14704835]

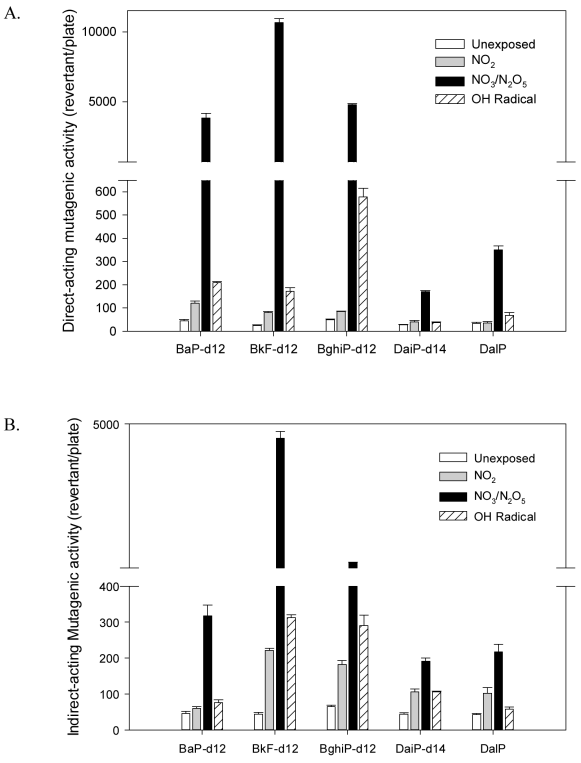

Figure 1.

Mean (± standard error) of A) direct-acting and B) indirect-acting mutagenicities (revertants/plate) of filter extracts. All extracts were tested in triplicate for mutagenic activity.

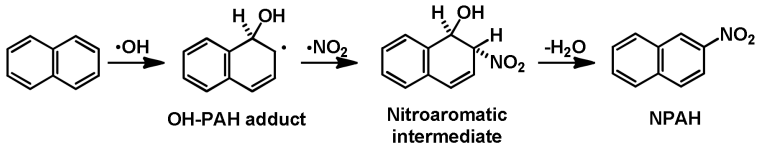

Scheme 1.

General mechanism for the nitration of PAHs via gas-phase reaction with OH radical.

Table 1

Free energies (ΔG_{rxn}) of OH-PAH adducts calculated using density functional theory (B3LYP) and the 6-31G(d) basis set, list of NPAHs measured in the laboratory studies, and whether or not the NPAH have been to date identified in the environment. The NPAH isomers are listed in order of predicted expected abundance.

PAH Studied	Numbering Scheme	Predicted OH-PAH-Adduct ΔG_{rxn} (Kcal/mol)	NPAH products identified in laboratory experiments	Laboratory exposures NPAH were identified in[±]	Previously detected in environment?
Benzo[a]pyrene	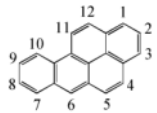	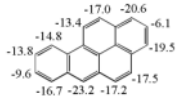	6-nitrobenzo[a]pyrene[ψ] 1-nitrobenzo[a]pyrene[*] 3-nitrobenzo[a]pyrene[*]	NO_2, NO_3/N_2O_5, OH NO_2, NO_3/N_2O_5, OH NO_2, NO_3/N_2O_5, OH	Y[17, 19, 20, 38] N N
Benzo[k]fluoranthene	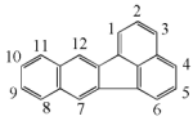	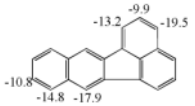	3-nitrobenzo[k]fluoranthene[*] 7-nitrobenzo[k]fluoranthene[θ] 8-nitrobenzo[k]fluoranthene[*] 1-nitrobenzo[k]fluoranthene[*] 9-nitrobenzo[k]fluoranthene[*] 3,7-dinitrobenzo[k]fluoranthene[θ] 4 dinitrobenzo[k]fluoranthenes[*]	NO_2, NO_3/N_2O_5, OH NO_2, NO_3/N_2O_5, OH NO_3/N_2O_5, OH NO_3/N_2O_5, OH NO_3/N_2O_5 NO_3/N_2O_5 NO_3/N_2O_5	N N N N N N N
Benzo[ghi]perylene	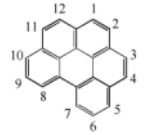	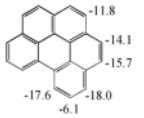	5-nitrobenzo[ghi]perylene[θ] 7-nitrobenzo[ghi]perylene[θ] 4-nitrobenzo[ghi]perylene[*]	NO_3/N_2O_5, OH NO_3/N_2O_5 NO_3/N_2O_5	N N N
Dibenzo[a,i]pyrene	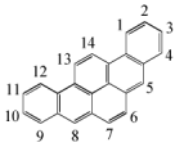	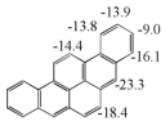	5-nitrodibenzo[a,i]pyrene[*]	NO_2, NO_3/N_2O_5	N
Dibenzo[a,l]pyrene	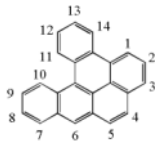	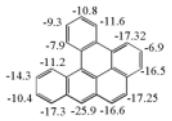	6-nitrodibenzo[a,l]pyrene[*]	NO_2, NO_3/N_2O_5, OH	N

[ψ]verified with deuterated standard.

$^{\theta}$ verified with non-deuterated standard.

$^{\pm}$ Perdeuterated forms were measured in the experiments.

* Not verified, no standards available.